

# Sternentstehung - Star Formation

Winter term 2022/2023

Henrik Beuther, Thomas Henning & Jonathan Henshaw

<i>18.10 Today: Introduction &amp; Overview</i>	<i>(Beuther)</i>
<i>25.10 Physical processes I</i>	<i>(Beuther)</i>
<i>08.11 Physical processes II</i>	<i>(Beuther)</i>
<i>15.11 Molecular clouds as birth places of stars</i>	<i>(Henshaw)</i>
<i>22.11 Molecular clouds (cont.), Jeans Analysis</i>	<i>(Henshaw)</i>
<b>29.11 Collapse models I</b>	<b>(Beuther)</b>
06.12 Collapse models II	(Henning)
13.12 Protostellar evolution	(Beuther)
20.12 Pre-main sequence evolution & outflows/jets	(Beuther)
10.01 Accretion disks I	(Henning)
17.01 Accretion disks II	(Henning)
24.01 High-mass star formation, clusters and the IMF	(Henshaw)
31.01 Extragalactic star formation	(Henning)
07.02 Planetarium@HdA, outlook, questions	(Beuther)
13.02 Examination week, no star formation lecture	

**Book: Stahler & Palla: The Formation of Stars, Wileys**

More Information and the current lecture files: [http://www.mpia.de/homes/beuther/lecture\\_ws2223.html](http://www.mpia.de/homes/beuther/lecture_ws2223.html)  
[beuther@mpia.de](mailto:beuther@mpia.de), [henning@mpia.de](mailto:henning@mpia.de) , [henshaw@mpia.de](mailto:henshaw@mpia.de)

# Last week

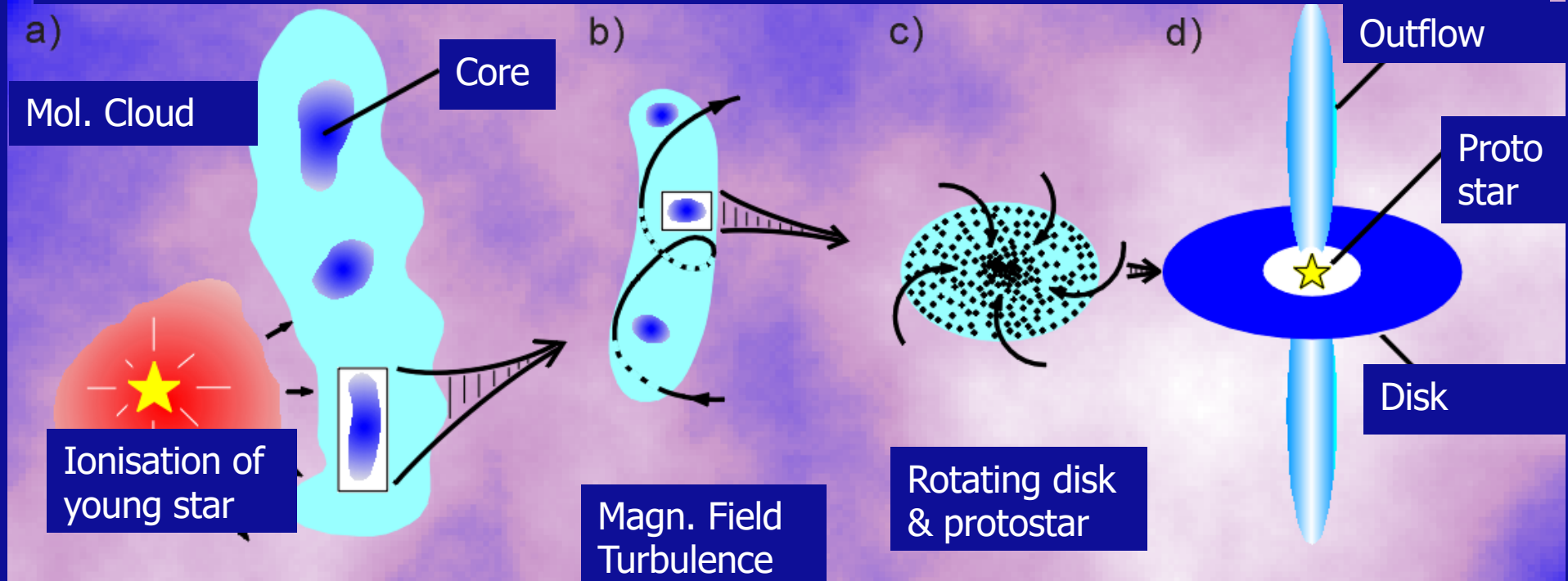
- Virial theorem and applications to cloud (in)stability
- Cloud lifetimes
- Jeans analysis and applications to fragmentation

# Topics today

- Isothermal sphere, hydrostatic equilibrium, grav. stability, Bonnor-Ebert spheres
- Rotational support
- Magnetic support and ambipolar diffusion
- Infall signatures

# Star formation paradigm

## Phases of star formation



<https://www.mpifr-bonn.mpg.de/473576/starform>

# Isothermal Sphere I

Three equations governing the equilibrium are:

Hydrostatic equilibrium

$$-\frac{1}{\rho}\nabla P - \nabla\Phi_g = 0 \quad (1)$$

Ideal isothermal gas

$$P = \rho a_t^2 \quad (2)$$

where the  $\Phi_g$  obeys Poisson equation

$$\nabla^2\Phi_g = 4\pi G\rho \quad (3)$$

Substituting equation 2 in 1 and after integration

$$\ln\rho + \Phi_g/a^2 = \text{const.} \quad (4)$$

In the spherical case, this is

$$\rho(r) = \rho_c \exp(-\Phi_g/a^2) \quad (5)$$

P: Pressure

$\rho$ : density

$\Phi_g$ : grav. Potential

$a_t$ : sound speed

# Isothermal Sphere II

With  $\rho_c$  the density at the center and  $\Phi_g(r=0) = 0$ ,  
the Poisson eq. becomes

$$\frac{1}{r^2} \frac{d}{dr} \left( r^2 \frac{d\Phi_g}{dr} \right) = 4\pi G \rho \quad (1)$$

$$= 4\pi G \rho_c \exp(-\Phi_g/a^2) \quad (2)$$

Often, this equations is used in dimensionless form  
with the dimensionless potential:

$$\phi = \Phi_g/a^2$$

and the dimensionless length  $\xi$

$$\xi = \sqrt{\frac{4\pi G \rho_c}{a^2}} r$$

Then the Poisson eq. turns into the Lane-Emden eq.

$$\frac{1}{\xi^2} \frac{d}{d\xi} \left( \xi^2 \frac{d\phi}{d\xi} \right) = \exp(-\phi) \quad (3)$$

Boundary conditions:

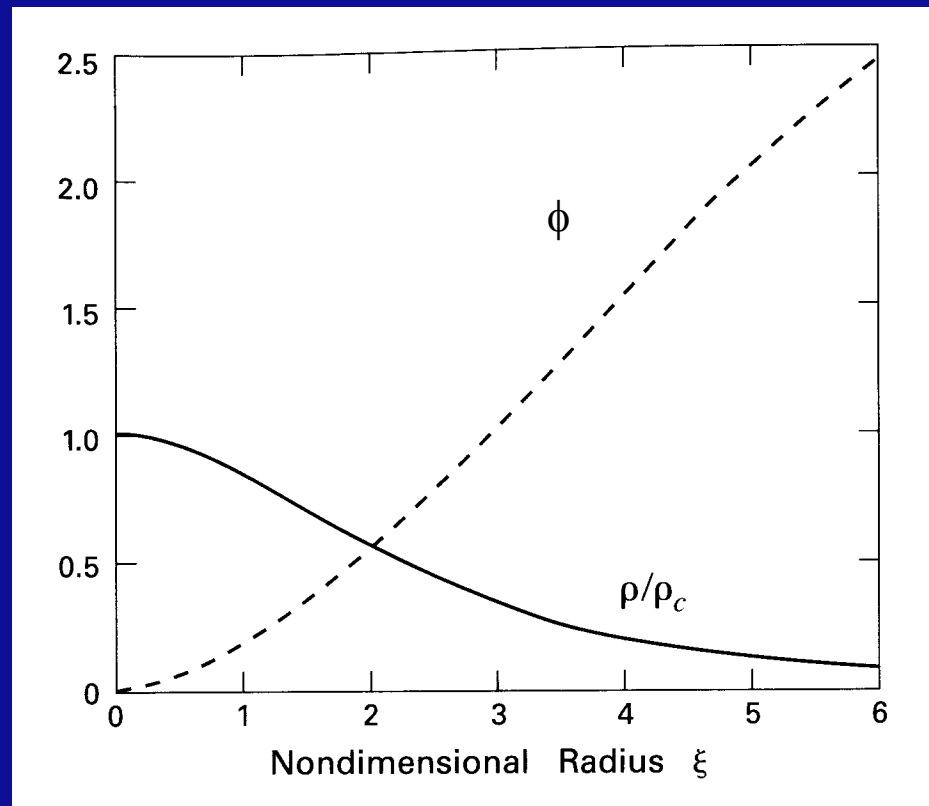
$$\phi(0) = 0$$

$$\phi'(0) = 0$$

Gravitational potential and  
force are 0 at the center.

→ Numerical integration: gravitational potential versus radius ... then density

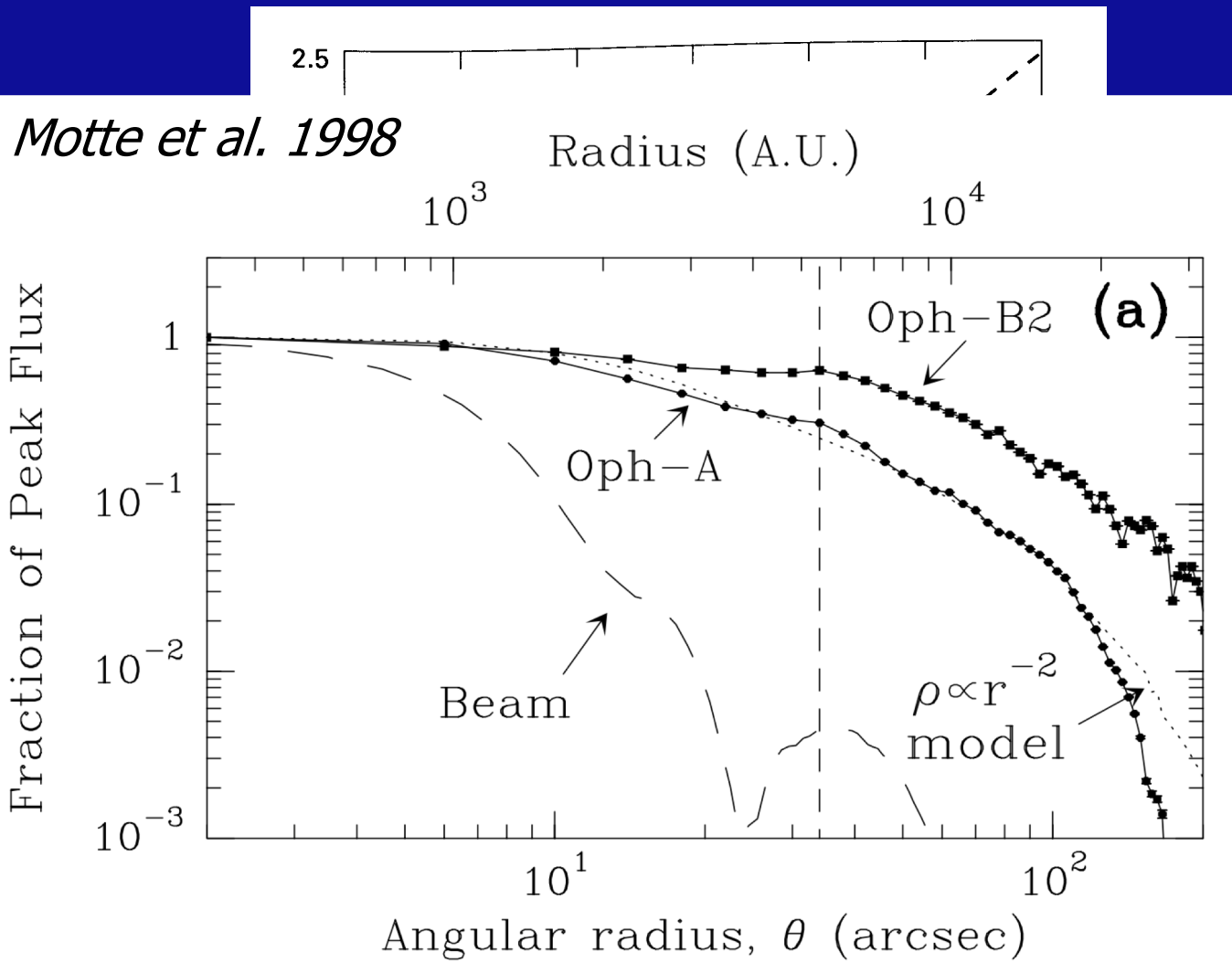
# Isothermal Sphere III



- Density and pressure ( $P=\rho a^2$ ) drop monotonically away from the center.
  - important to offset inward pull from gravity for grav. collapse.
- After numerical integration of the Lane-Emden equation
  - density  $\rho/\rho_c$  approaches asymptotically  $2/\xi^2$ .
- Hence the dimensional density profile of the isothermal sphere is:

$$\rho(r) = a^2/(2\pi G r^2) \sim 1/r^2.$$

# Isothermal Sphere III



- Densi
- After

the center.  
collapse.

→ density  $\rho/\rho_c$  approaches asymptotically  $2/\xi^2$ .

- Hence the dimensional density profile of the isothermal sphere is:

$$\rho(r) = a^2/(2\pi Gr^2) \sim 1/r^2.$$



# Isothermal Sphere IV

The dimensional mass is

$$M = 4\pi \int_0^{r_0} \rho r^2 dr \quad (1)$$

$$= 4\pi \rho_c \left( \frac{a_t^2}{4\pi G \rho_c} \right)^{3/2} \int_0^{\xi_0} e^{-\phi} \xi^2 d\xi \quad (2)$$

Using the Lane-Emden eq. and the boundary condition  $\phi'(0) = 0$

$$\rightarrow M = 4\pi \rho_c \left( \frac{a_t^2}{4\pi G \rho_c} \right)^{3/2} \left( \xi^2 \frac{d\phi}{d\xi} \right)_{\xi_0} \quad (3)$$

Defining furthermore a dimensionless mass  $m$

$$m = \frac{P_0^{1/2} G^{3/2} M}{a_t^4}, \text{ with } P_0 = \rho_0 a_t^2 \quad (4)$$

the dimensionless mass equals

$$m = \left( 4\pi \frac{\rho_c}{\rho_0} \right)^{-1/2} \left( \xi^2 \frac{d\phi}{d\xi} \right)_{\xi_0} \quad (5)$$

Since  $\xi_0$  is known for each  $\rho_c/\rho_0$ , and  $\left( \xi^2 \frac{d\phi}{d\xi} \right)_{\xi_0}$  can be read from the previous figure, one can evaluate  $m$ .

With:

$$r = \sqrt{(a_t^2/(4\pi G \rho_c))} * \xi$$

$$\rho = \rho_c \exp(-\phi)$$

Subscript 0 at cloud edge

# Isothermal Sphere IV

The dimensional mass is

$$M = 4\pi \int_0^{r_0} \rho r^2 dr \quad (1)$$

$$= 4\pi \rho_c \left( \frac{a_t^2}{4\pi G \rho_c} \right)^{3/2} \int_0^{\xi_0} e^{-\phi} \xi^2 d\xi \quad (2)$$

With:

$$r = \sqrt{(a_t^2 / (4\pi G \rho_c))} * \xi$$

$$\rho = \rho_c \exp(-\phi)$$

Subscript 0 at cloud edge

Using the Lane-Emden eq. and the boundary condition  $\phi'(0) = 0$

$$\rightarrow M = 4\pi \rho_c \left( \frac{a_t^2}{4\pi G \rho_c} \right)^{3/2} \left( \xi^2 \frac{d\phi}{d\xi} \right)_{\xi_0}$$

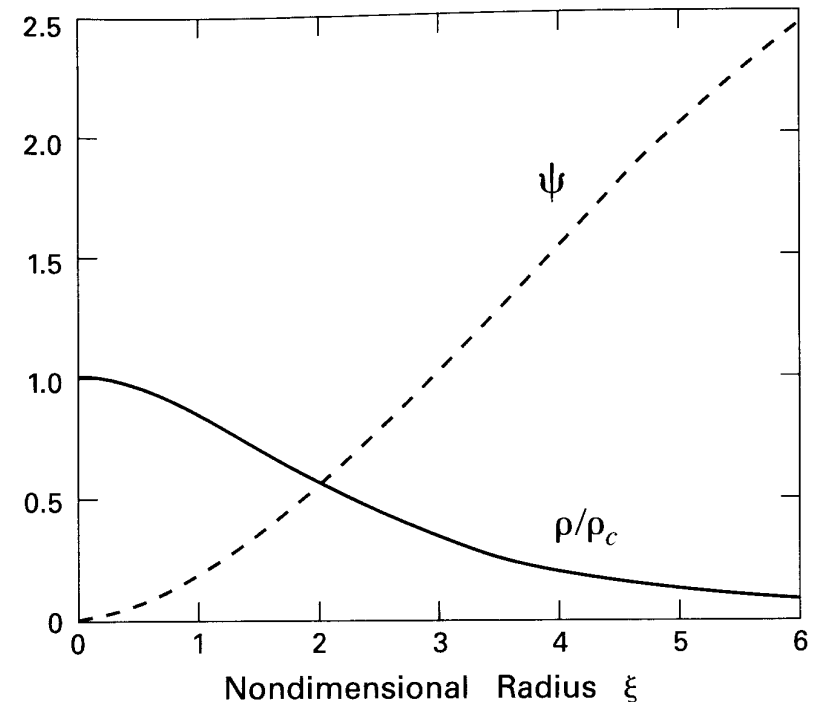
Defining furthermore a dimensionless mass

$$m = \frac{P_0^{1/2} G^{3/2} M}{a_t^4}, \text{ with } P_0 = \rho_0 a_t^2$$

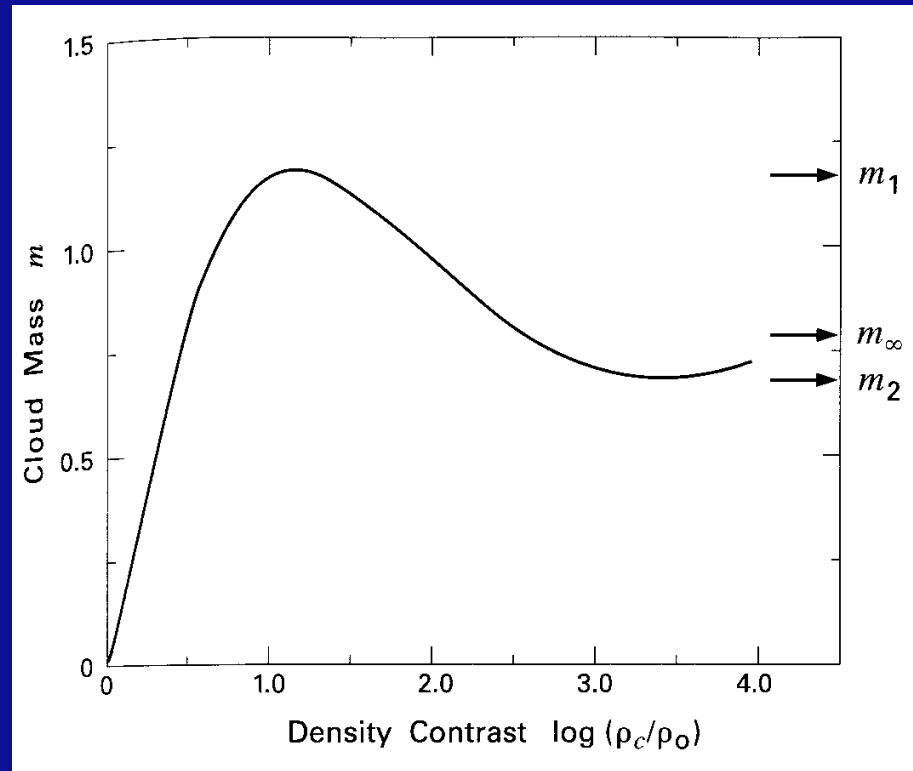
the dimensionless mass equals

$$m = \left( 4\pi \frac{\rho_c}{\rho_0} \right)^{-1/2} \left( \xi^2 \frac{d\phi}{d\xi} \right)_{\xi_0}$$

Since  $\xi_0$  is known for each  $\rho_c/\rho_0$ , and  $\left( \xi^2 \frac{d\phi}{d\xi} \right)_{\xi_0}$  can be read from the previous figure, one can evaluate  $m$ .



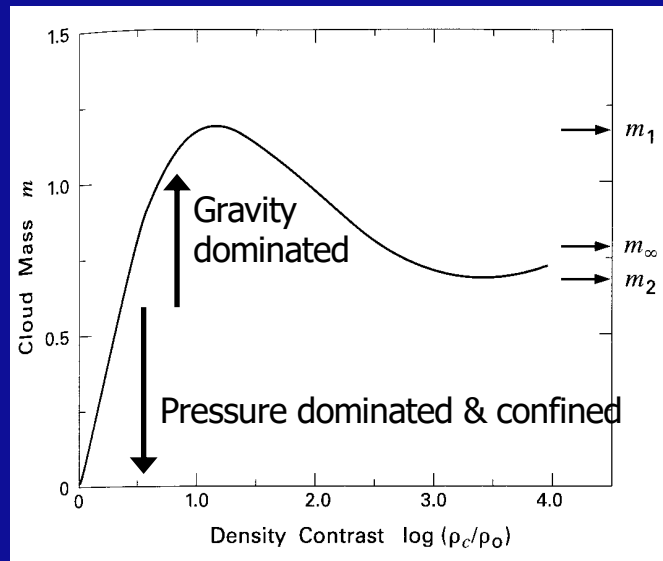
# Isothermal Sphere V



The beginning is for a radius  $\xi_0=0$ , hence  $\rho_c/\rho_0=1$  and  $m=0$ .

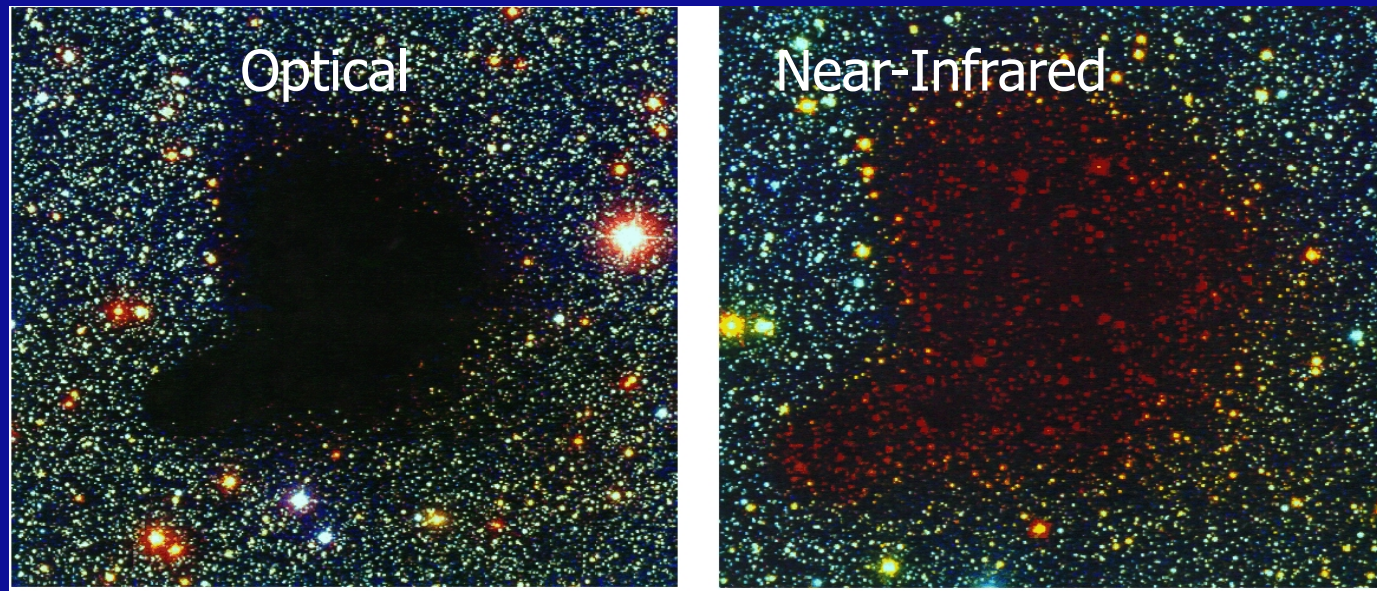
For increasing  $\rho_c/\rho_0$ ,  $m$  (and  $\Phi$ ) increases until  $\rho_c/\rho_0=14.1$ , corresponding to the dimensionless radius  $\xi_0=6.5$ .

# Gravitational stability

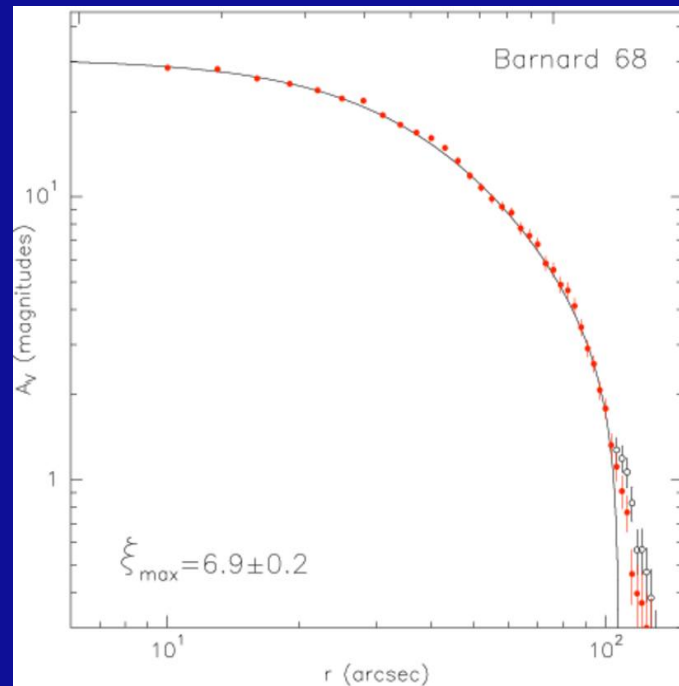


- Low density-contrast cloud: Increasing outer pressure  $P_0 \rightarrow$  rise of  $m$  &  $\rho_c/\rho_0$ .
- With internal pressure  $P = \rho a_t^2$  and  $\rho \sim 1/r^2$  decreasing outward  $\rightarrow$  inner  $P$  rises more strongly than  $P_0 \rightarrow$  cloud remains stable.
- High-density contrast: following the Boyle-Mariotte law for an ideal gas:
  - $PV = \text{const} \rightarrow P * 4/3\pi r^3 = \text{const}$
  - $\rightarrow$  core shrinks with increasing outer pressure  $P_0$ .
- All clouds with  $\rho_c/\rho_0 > 14.1$  ( $\xi_0 = 6.5$ ) are gravitationally unstable, the critical mass is the Bonnor-Ebert mass (eq. 4, 2 slides ago, Ebert 1955, Bonnor 1956)
  - $M_{BE} = (m_1 a_t^4) / (P_0^{1/2} G^{3/2})$

# Gravitational stability: The case of B68



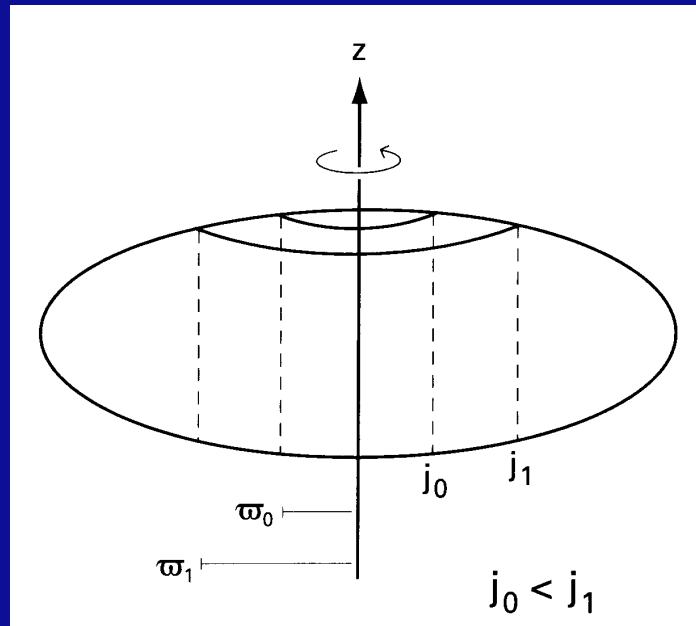
$\xi_0=6.9$  is only marginally about the critical value 6.5  
→ gravitational stable or at the verge of collapse



# Topics today

- Isothermal sphere, hydrostatic equilibrium, grav. stability, Bonnor-Ebert spheres
- **Rotational support**
- Magnetic support and ambipolar diffusion
- Infall signatures

# Basic rotational configurations I



Adding a centrifugal potential  $\Phi_{\text{cen}}$ , the hydrodynamic equation reads  

$$-1/\rho \text{ grad}(P) - \text{grad}(\Phi_g) - \text{grad}(\Phi_{\text{cen}}) = 0$$

With  $\Phi_{\text{cen}}$  defined as

$$\Phi_{\text{cen}} = - \int (j^2/\omega^3) d\omega$$

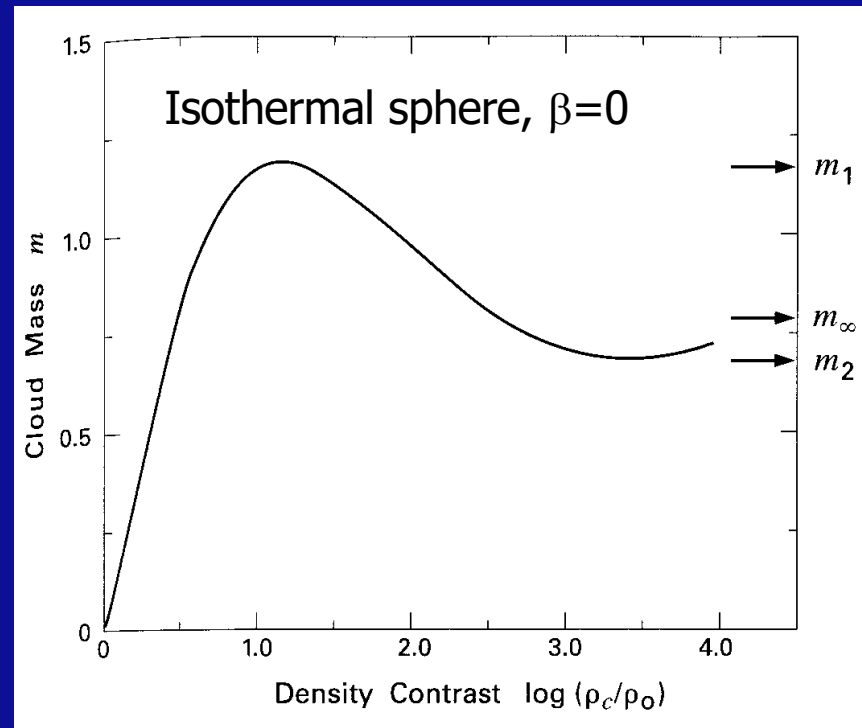
$j$ : specific angular momentum

$\omega$ : cylindrical radius

and  $j = \omega u$  with  $u$  the velocity around the rotation axis

Rotation flattens cores and may be additional support against collapse.

# Basic rotational configurations II



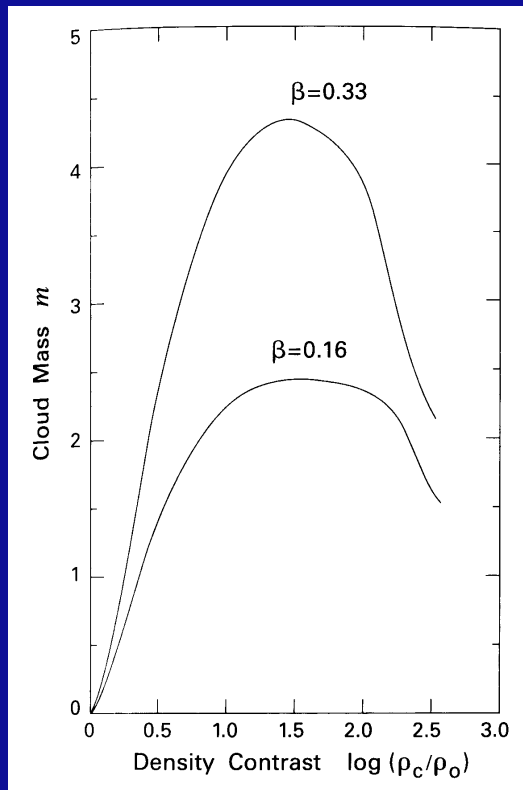
Compared to previous Bonnor-Ebert models, these rotational models have (in addition to the density contrast  $\rho_c/\rho_0$ ) the parameter  $\beta$  quantifying the degree of rotation.  $\beta$  defined as ratio of rotational to gravitational energy:

$$\beta = T_{\text{rot}}/W$$

$\beta > 1/3$  corresponds to breakup speed of the cloud. So  $0 < \beta < 1/3$



# Basic rotational configurations III



In realistic clouds, for flattening to appear, the rotational energy has to be at least 10% of the gravitational energy.  $T_{\text{rot}}/W$  equals approximately  $\beta$ .

Examples:

$$T_{\text{rot}} \approx I\Omega^2 = mr^2\Omega^2$$

( $I$ : moment of inertia,  $\Omega$ : rotational velocity)

$$W \approx Gm^2/r$$

$$\rightarrow T_{\text{rot}}/W \approx 1 \times 10^{-3} (\Omega/(1 \text{ km s}^{-1} \text{ pc}^{-1}))^2 (r/(0.1 \text{ pc}))^3 (m/(10 M_{\text{sun}}))^{-1}$$

GMCs: Velocity gradient of 0.05 km/s representing solid body rotation,  $200 M_{\text{sun}}$  and 2 pc size imply also  $T_{\text{rot}}/W \sim 10^{-3}$  (similar values for dense cores)

→ Cloud elongations do not arise from rotation, and centrifugal force NOT sufficient for cloud stability!

Other stability factors are necessary --> Magnetic fields

# Specific angular momentum

Specific angular momentum  $j=J/M$  is reduced from molecular cloud to star.

	$J/M(\text{cm}^2/\text{s})$
Molecular clump	$10^{23}$
Binary ( $P\sim 10^4\text{yr}$ )	$4\times 10^{20}-10^{21}$
Binary ( $P\sim 10\text{yr}$ )	$4\times 10^{19}-10^{20}$
Binary ( $P\sim 3\text{d}$ )	$4\times 10^{18}-10^{19}$
T Tauri star	$10^{17}$
Sun	$10^{15}$

→ Specific angular momentum needs to be reduced by 6 orders of magnitude from molecular cloud to T Tauri star scale.

# Topics today

- Isothermal sphere, hydrostatic equilibrium, grav. stability, Bonnor-Ebert spheres
- Rotational support
- **Magnetic support and ambipolar diffusion**
- Infall signatures

# Magnetic fields I

The equation for magneto-hydrodynamic equilibrium now:

$$-1/\rho \text{ grad}(P) - \text{grad}(\Phi_g) - 1/(\rho c) \mathbf{j} \times \mathbf{B} = 0$$

Numerical solving → solutions with 3 free parameters:

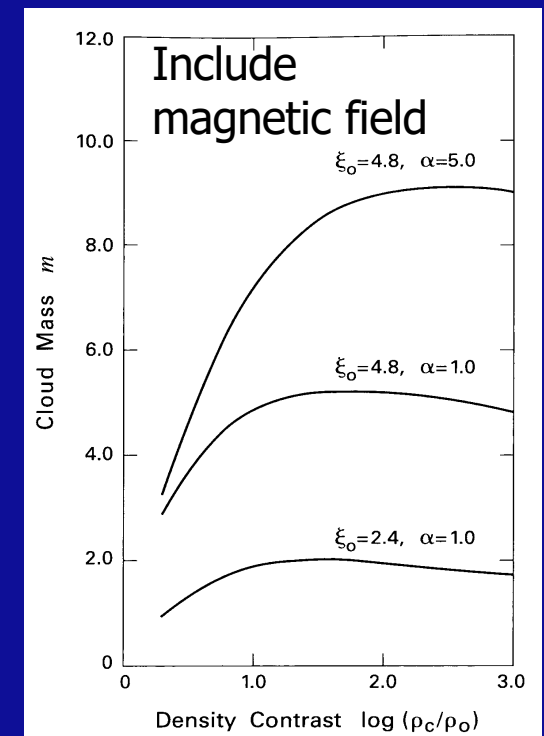
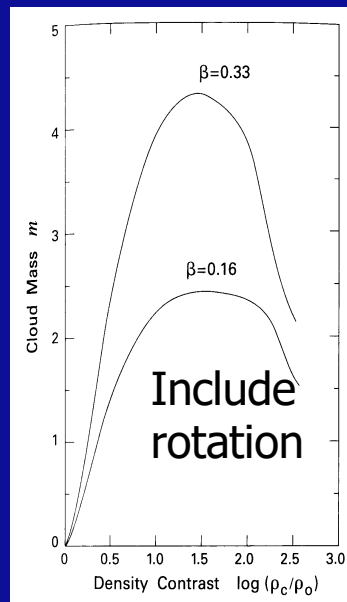
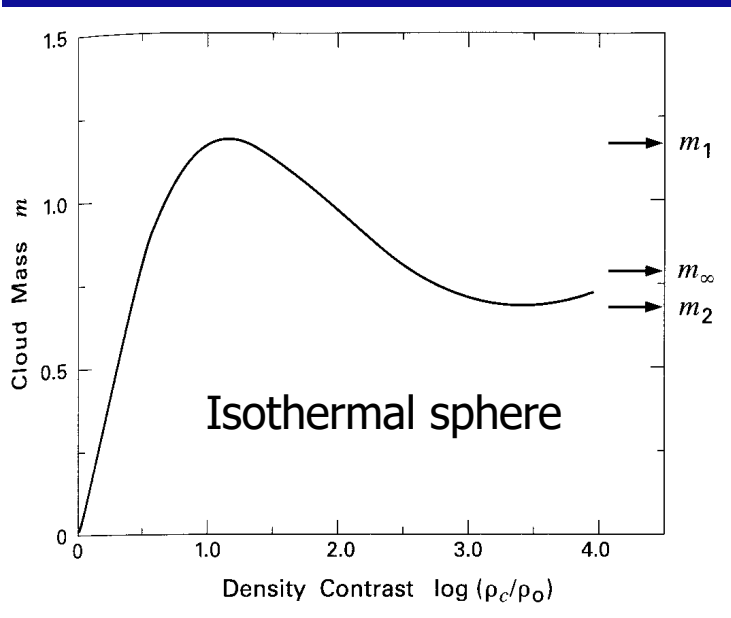
the density contrast ratio  $\rho_c/\rho_0$ ,

the ratio  $\alpha$  between magnetic to thermal pressure

$$\alpha = B_0^2/(8\pi P_0)$$

and the dimensionless radius of the initial sphere

$$\xi_0 = (4\pi G\rho_0/a_t^2)^{1/2} * R_0$$



Fit to numerical results:  $m_{\text{crit}} = 1.2 + 0.15 \alpha^{1/2} \xi_0^2$

# Magnetic fields II

Conversion to dimensional form (multiply by  $a_t^4/(P_0^{1/2}G^{3/2})$ ):

→ first term equals the Bonnor-Ebert Mass ( $M_{BE} = m_1 a_t^4/(P_0^{1/2}G^{3/2})$ )

$$M_{crit} = M_{BE} + M_{magn}$$

$$\begin{aligned} \text{with } M_{magn} &= 0.15 \alpha^{1/2} \xi_0^2 a_t^4/(P_0^{1/2}G^{3/2}) \\ &= 0.15 \frac{2}{\sqrt{2\pi}} (B_0 \pi R_0^2/G^{1/2}) \propto B_0 \end{aligned}$$

--> magnetic mass  $M_{magn}$  proportional to the B-field!

Qualitative difference between purely thermal clouds and magnetized clouds.

If increase of outer pressure  $P_0$  around core of mass  $M$

→ Bonnor-Ebert mass decreases until  $M_{BE} < M$  → then cloud collapse

However, in magnetic case: if  $M < M_{magn}$  → cloud remains stable because  $M_{magn}$  is constant as long a flux-freezing applies.

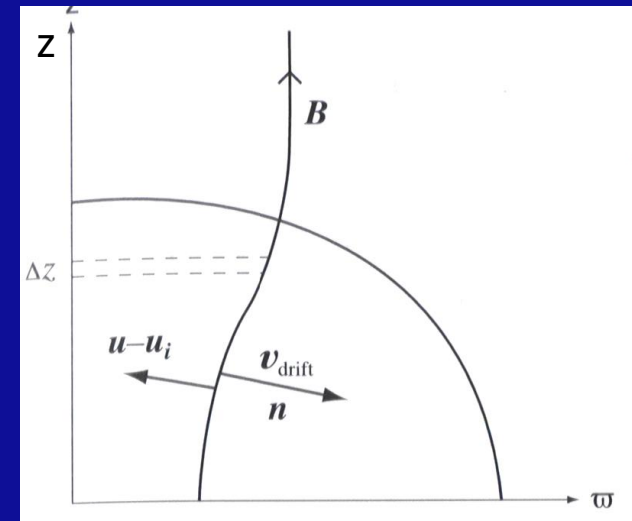
# Ambipolar diffusion I

- Lower density GMCs, large ionization degree  $\rightarrow$  ions & neutrals strongly collisionally coupled.
- Dense cores: lower ionization degree  $\rightarrow$  neutrals & ions easier decouple.

Neutrals stream through ions accelerated by gravity.

$\rightarrow$  drag force between ions & neutrals from collisions.

- Furthermore, Lorentz force acts on ions.



- Drift velocity between ions and neutrals:  $v_{\text{drift}} = v_i - v_n$
- Drag force between ions and neutrals is:  $F_{\text{drag}} = n_n \langle \sigma_{\text{in}} v_{\text{drift}} \rangle m_n v_{\text{drift}}$   
(average number of collision per unit time  $n_n \langle \sigma_{\text{in}} v_{\text{drift}} \rangle$  times the transferred momentum  $m_n v_{\text{drift}}$ )
- $\rightarrow$  equation of motion with drag & Lorentz force:

$$n_i F_{\text{drag}} = \mathbf{j} \times \mathbf{B} / c = 1/(4\pi) (\text{rot } \mathbf{B}) \times \mathbf{B}$$

(with Ampere's law:  $\text{rot } \mathbf{B} = 4\pi/c * \mathbf{j}$ )

$$\rightarrow v_{\text{drift}} = (\text{rot } \mathbf{B}) \times \mathbf{B} / (4\pi n_i n_n m_n \langle \sigma_{\text{in}} v_{\text{drift}} \rangle)$$

$n_n$ : neutral density  
 $n_i$ : number of ions  
 $\sigma_{\text{in}}$ : ion-neutral cross section  
 $m_n$ : mass of neutral

# Ambipolar diffusion II

Dense core with size  $L \rightarrow$  time-scale for ambipolar diffusion:

$$t_{\text{ad}} = L/|v_{\text{drift}}| = (4\pi n_i n_n m_n \langle \sigma_{\text{in}} v_{\text{drift}} \rangle) L / (|(\text{rot } \mathbf{B}) \times \mathbf{B}|)$$

Approximating  $(\text{rot } \mathbf{B} = B/L)$ :  $|(\text{rot } \mathbf{B}) \times \mathbf{B}| = B^2/L$

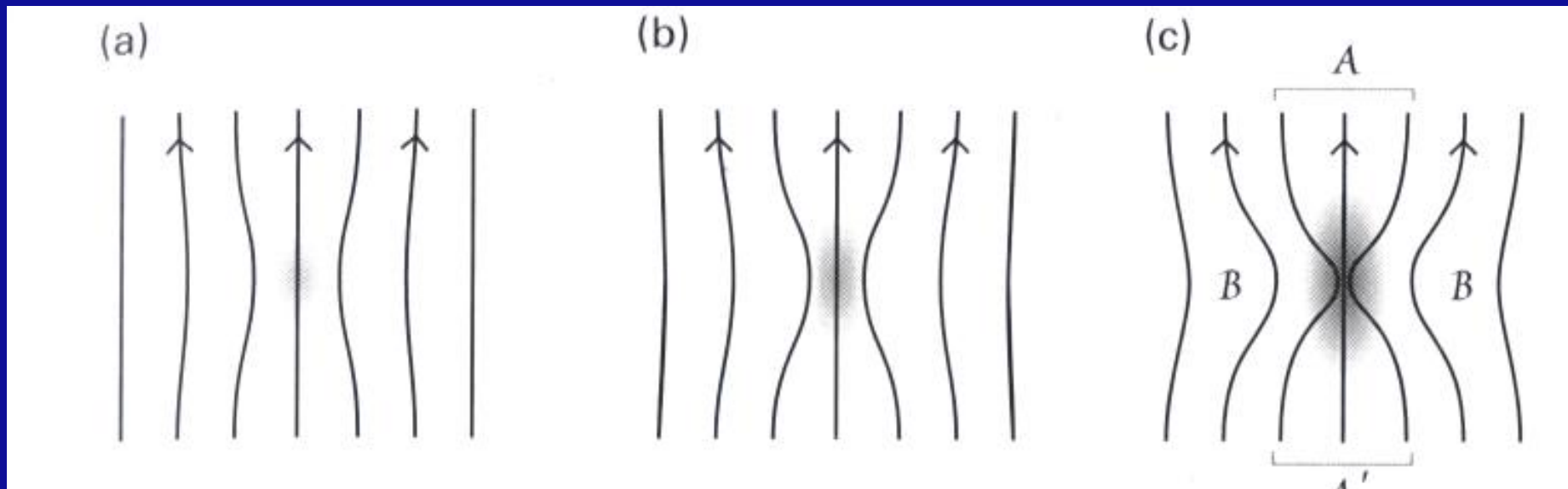
$$\rightarrow t_{\text{ad}} = (4\pi n_i n_n m_n \langle \sigma_{\text{in}} v_{\text{drift}} \rangle) L^2 / B^2$$

$\rightarrow$  ambipolar diffusion time-scale proportional to:  
ionization degree, density & size of the cloud; inversely prop. to mag. field

$$\rightarrow t_{\text{ad}} \approx 3 \times 10^6 \text{yr} (n_{\text{H}_2}/10^4 \text{cm}^{-3})^{3/2} (B/30 \mu\text{G})^{-2} (L/0.1 \text{pc})^2$$

Still under discussion whether this time-scale sets the star formation rate or whether it is too slow and other processes like turbulence are required.

# Ambipolar diffusion caveat

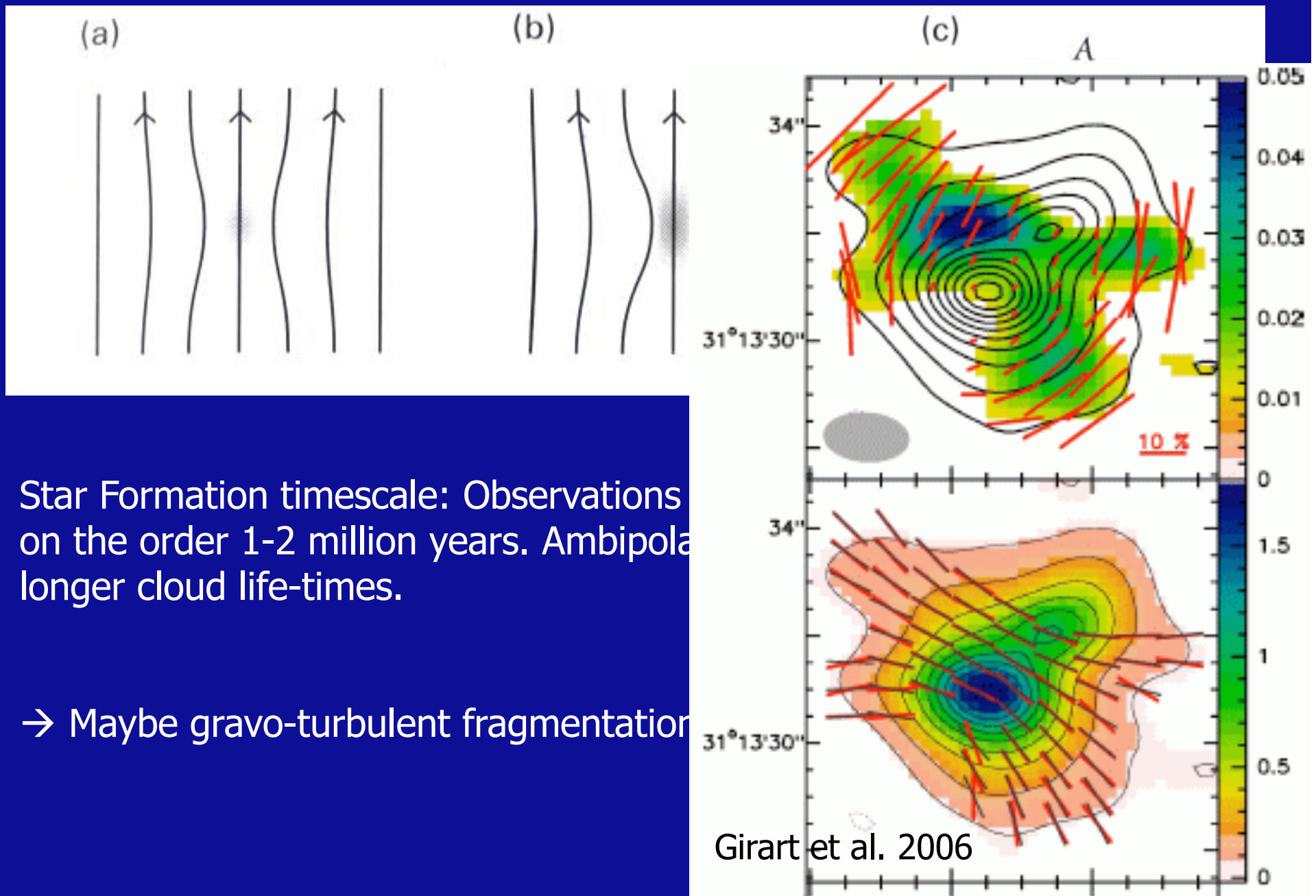


Star Formation timescale: Observations indicate rapid star formation on the order 1-2 million years. Ambipolar diffusion usually requires longer cloud life-times.

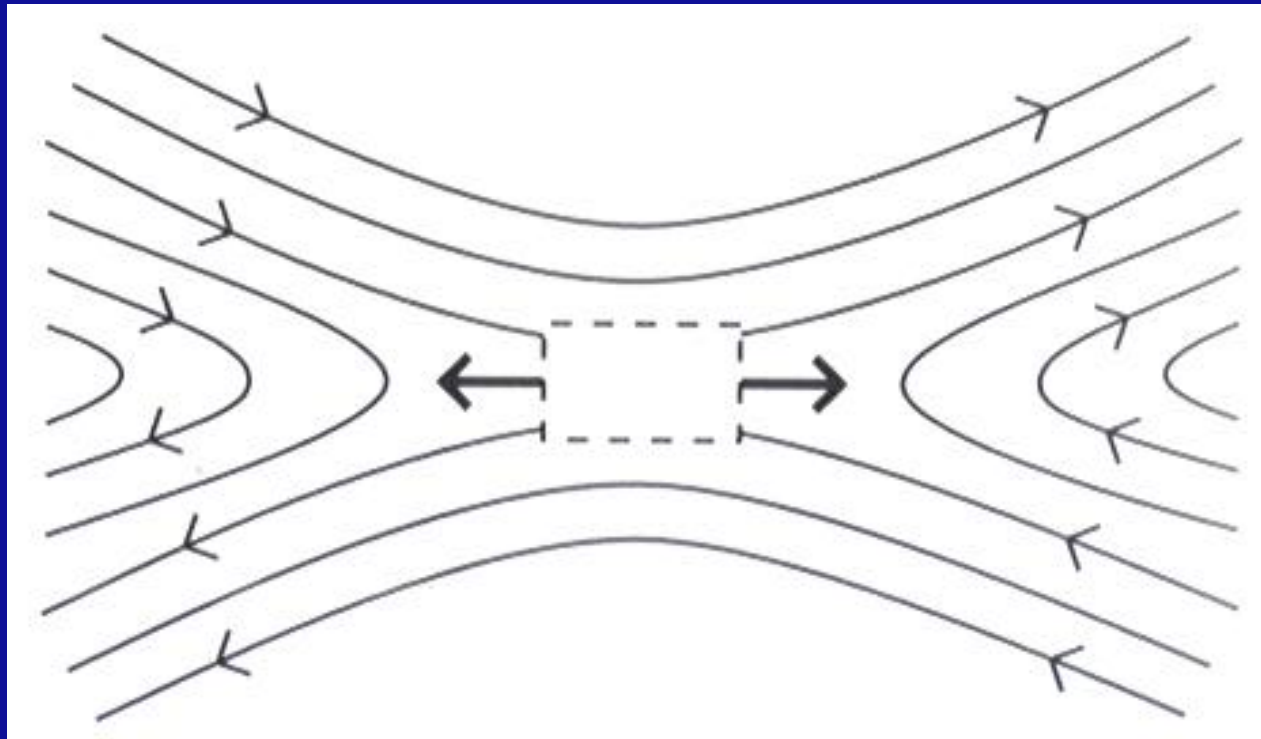
→ Maybe gravo-turbulent fragmentation necessary ...



# Ambipolar diffusion caveat



# Magnetic reconnection

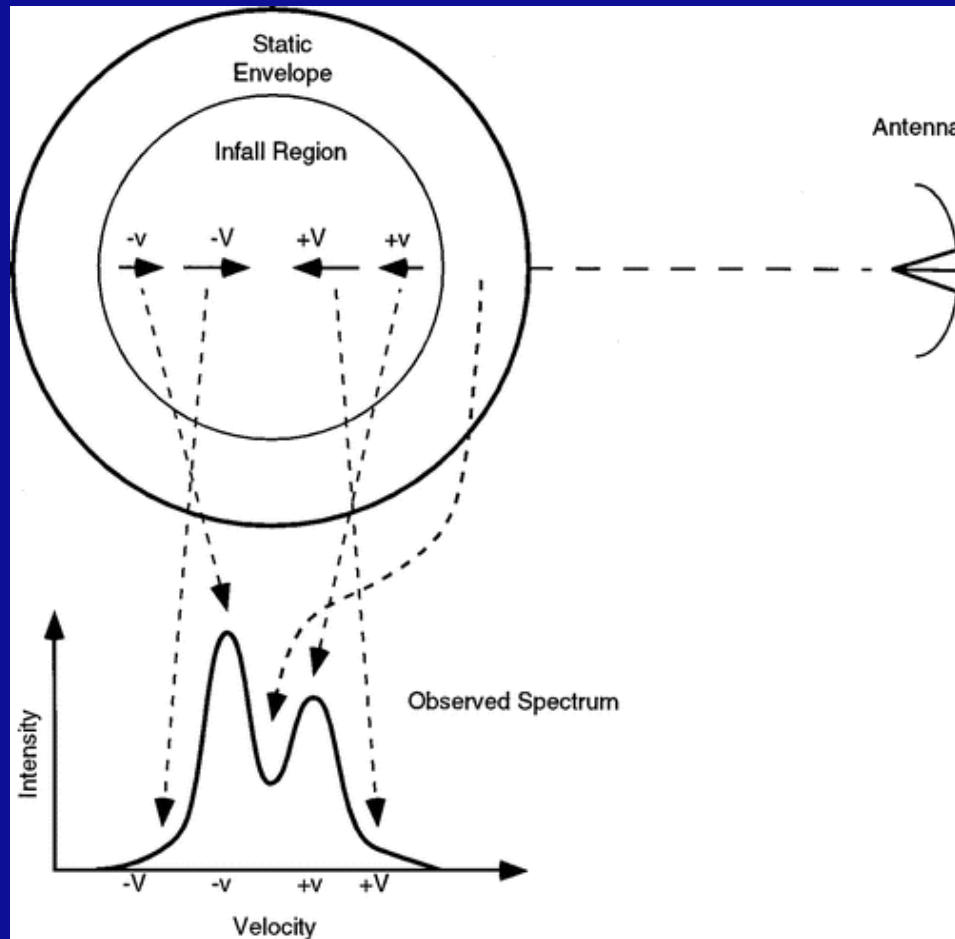


- Field lines of opposite direction are dragged together.
  - antiparallel B field lines annihilate and
  - magnetic energy dissipates as heat.
- This process was first invoked to explain large luminosities observed in solar flares.

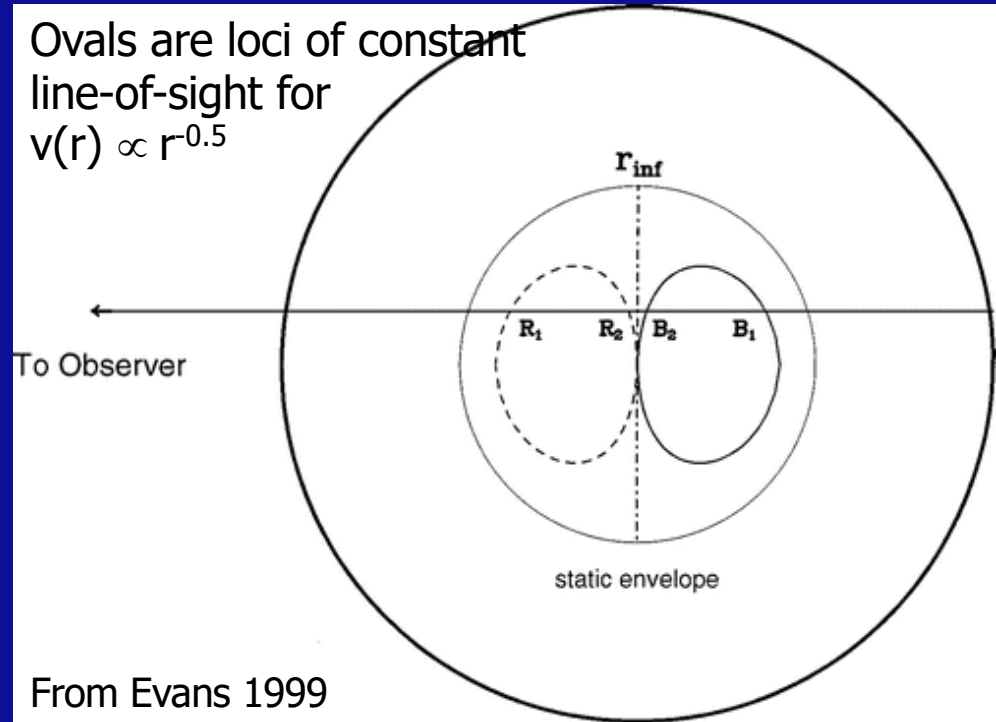
# Topics today

- Isothermal sphere, hydrostatic equilibrium, grav. stability, Bonnor-Ebert spheres
- Rotational support
- Magnetic support and ambipolar diffusion
- Infall signatures

# Infall signatures I



Ovals are loci of constant line-of-sight for  $v(r) \propto r^{-0.5}$



From Evans 1999

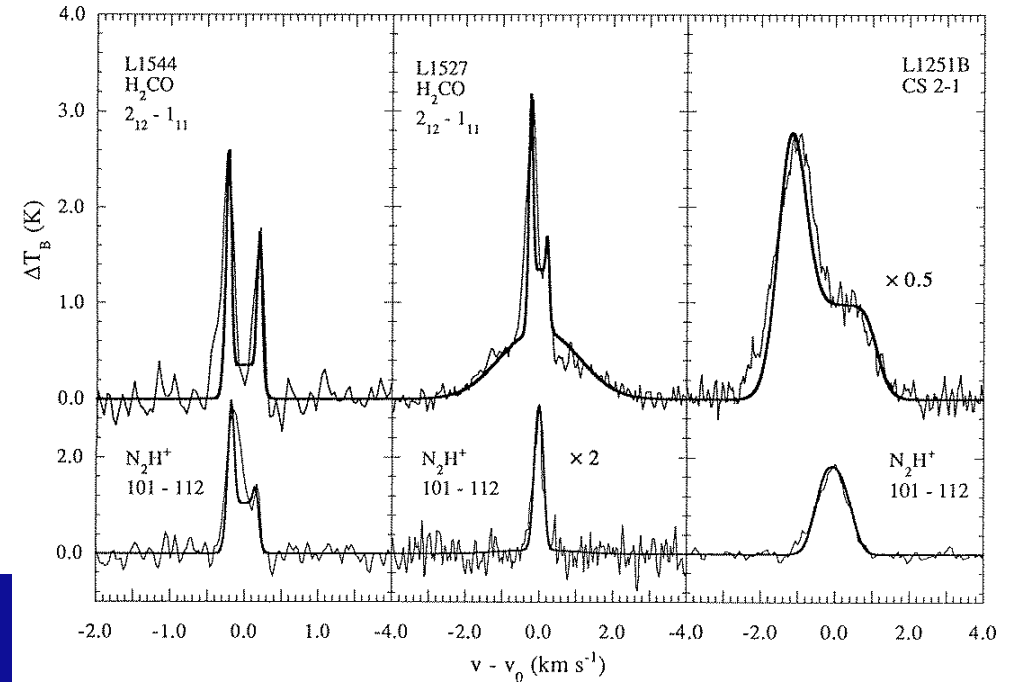
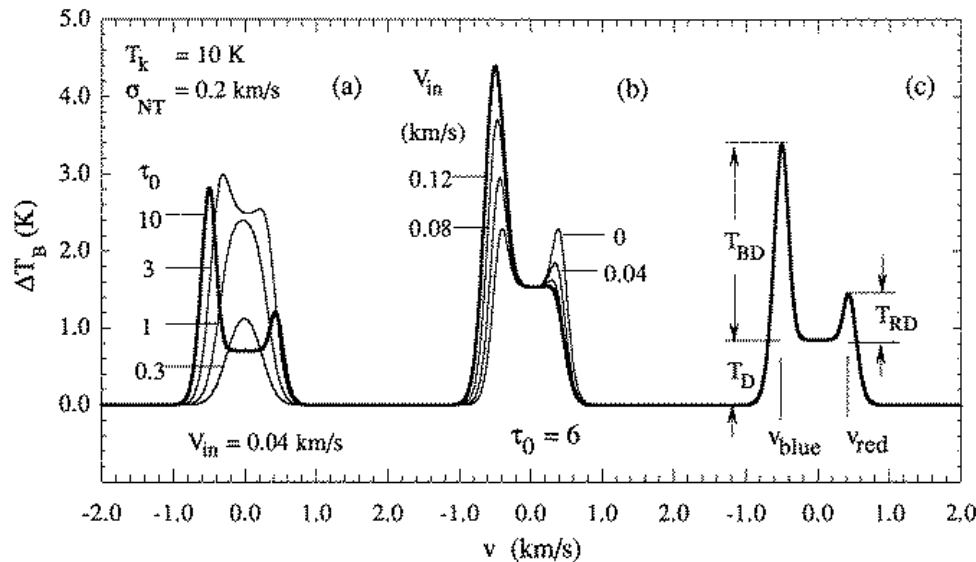
1. Rising  $T_{ex}$  along line of sight
2. Velocity gradient
3. Line optically thick
4. An additional optically thin line peaks at center

# Infall signatures II

Models

Spectra and fits

(Myers et al. 1996)



Model with two uniform regions along the line of sight with velocity dispersion  $\sigma$  and peak optical depth  $\tau_0 \rightarrow$  infall velocity  $v_{in}$ :

$$v_{in} \approx \sigma^2 / (v_{red} - v_{blue}) * \ln((1 + \exp(T_{BD}/T_D)) / (1 + \exp(T_{RD}/T_D)))$$

In low-mass regions  $v_{in}$  is usually of the order 0.1 km/s. In high-mass regions  $V_{in}$  can exceed 1 km/s and hence be supersonic.

# Summary

- Hydrostatic equilibrium between thermal pressure and gravitational force.
  - Bonner Ebert mass for gravitationally stable cores.
  
- Can rotation support cloud stability?
  
- Magnetic cloud support and ambipolar diffusion
  
- Observational signatures of infall motions

# Sternentstehung - Star Formation

Winter term 2022/2023

Henrik Beuther, Thomas Henning & Jonathan Henshaw

<i>18.10 Today: Introduction &amp; Overview</i>	<i>(Beuther)</i>
<i>25.10 Physical processes I</i>	<i>(Beuther)</i>
<i>08.11 Physical processes II</i>	<i>(Beuther)</i>
<i>15.11 Molecular clouds as birth places of stars</i>	<i>(Henshaw)</i>
<i>22.11 Molecular clouds (cont.), Jeans Analysis</i>	<i>(Henshaw)</i>
<i>29.11 Collapse models I</i>	<i>(Beuther)</i>
<b>06.12 Collapse models II</b>	<b>(Henning)</b>
13.12 Protostellar evolution	(Beuther)
20.12 Pre-main sequence evolution & outflows/jets	(Beuther)
10.01 Accretion disks I	(Henning)
17.01 Accretion disks II	(Henning)
24.01 High-mass star formation, clusters and the IMF	(Henshaw)
31.01 Extragalactic star formation	(Henning)
07.02 Planetarium@HdA, outlook, questions	(Beuther)
13.02 Examination week, no star formation lecture	

**Book: Stahler & Palla: The Formation of Stars, Wileys**

More Information and the current lecture files: [http://www.mpia.de/homes/beuther/lecture\\_ws2223.html](http://www.mpia.de/homes/beuther/lecture_ws2223.html)  
[beuther@mpia.de](mailto:beuther@mpia.de), [henning@mpia.de](mailto:henning@mpia.de) , [henshaw@mpia.de](mailto:henshaw@mpia.de)

# Heidelberg Joint Astronomical Colloquium

Winter Semester 2022 — Tuesday November 29th, 16:00

Main Lecture Theatre, Philosophenweg 12

**Dylan Nelson (Institut für Theoretische Astrophysik)**

## **The connection(s) between galaxies and their gaseous halos**



Caption: Gas motion on Mpc scales around a halo

Those unable to attend the colloquium in person are invited to participate online through Zoom.

More information is given on HePhySTO: <https://www.physik.uni-heidelberg.de/hephysto/>

---